

An epidemiological stochastic predator-prey model with prey refuge and harvesting

Israr Ali, Hui Zhang(张慧), Syed Murad Ali Shah, Abdulwasea Alkhazzan, and Yassine Sabbar
Citation: Chin. Phys. B, 2026, 35 (**2**): 020503. DOI: 10.1088/1674-1056/adf17f
http://cpb.iphy.ac.cn; http://iopscience.iop.org/cpb

What follows is a list of articles you may be interested in

Visibility graph approach to extreme event series

Jing Zhang(张晶), Xiaolu Chen(陈晓露), Haiying Wang(王海英), Changgui Gu(顾长贵), and Huijie Yang(杨会杰)
Chin. Phys. B, 2023, 32 (**10**): 100505. DOI: 10.1088/1674-1056/acd62b

Dynamical analysis for the sustained harvesting of microorganisms using flocculants in a random environment

Rong Liu(刘蓉) and Wanbiao Ma(马万彪)
Chin. Phys. B, 2023, 32 (**5**): 050502. DOI: 10.1088/1674-1056/ac9367

Broadband energy harvesting based on one-to-one internal resonance

Wen-An Jiang(姜文安), Xin-Dong Ma(马新东), Xiu-Jing Han(韩修静)†, Li-Qun Chen(陈立群), and Qin-Sheng Bi(毕勤胜)
Chin. Phys. B, 2020, 29 (**10**): 100503. DOI: 10.1088/1674-1056/aba5fd

Active Brownian particles simulated in molecular dynamics

Liya Wang(王丽雅), Xinpeng Xu(徐新鹏), Zhigang Li(李志刚), Tiezheng Qian(钱铁铮)
Chin. Phys. B, 2020, 29 (**9**): 090501. DOI: 10.1088/1674-1056/aba60d

Prompt efficiency of energy harvesting by magnetic coupling of an improved bi-stable system

Hai-Tao Li(李海涛), Wei-Yang Qin(秦卫阳)
Chin. Phys. B, 2016, 25 (**11**): 110503. DOI: 10.1088/1674-1056/25/11/110503

An epidemiological stochastic predator–prey model with prey refuge and harvesting

Israr Ali[1], Hui Zhang(张慧)[1,2,3,‡], Syed Murad Ali Shah[4], Abdulwasea Alkhazzan[5,†], and Yassine Sabbar[6]

[1] *School of Mathematics and Statistics, Northwestern Polytechnical University, Xi'an* 710072, *China*
[2] *Shenzhen Research Institute of Northwestern Polytechnical University, Shenzhen* 518057, *China*
[3] *International Joint Research Center on Operations Research, Optimization and Artificial Intelligence, Xi'an* 710072, *China*
[4] *School of Statistics, Southwestern University of Finance and Economics, Chengdu* 610074, *China*
[5] *School of Information Engineering, Xi'an Fanyi University, Xi'an* 710105, *China*
[6] *IMIA Laboratory, T-IDMS, FST Errachidia, Moulay Ismail University of Meknes, P.O. Box* 509, 52000, *Boutalamine, Errachidia, Morocco*

(Received 21 May 2025; revised manuscript received 13 July 2025; accepted manuscript online 18 July 2025)

Predator–prey interactions are fundamental to understanding ecosystem stability and biodiversity. In this study, we propose and analyze a stochastic predator–prey model that incorporates two critical ecological factors: prey refuge and harvesting. The model also integrates disease transmission within the predator population, adding an important layer of realism. Using rigorous mathematical techniques, we demonstrate the existence and uniqueness of a global positive solution, thereby confirming the model's biological feasibility. We further derive sufficient conditions for two key ecological scenarios: stochastic permanence, which ensures the sustained co-existence of prey and predators over time, and extinction, where one or both populations decline to zero. The interplay between prey refuge and harvesting is thoroughly examined to understand their combined impact on population dynamics. All theoretical results are validated by detailed numerical simulations, highlighting the applicability of the model to real-world ecological systems. From the simulation results, we observed that with an adequate level of prey refuge and predator harvesting, the susceptible predator and prey co-exist with extensive oscillations, while the infected predator population was moving towards extinction. In addition, we have investigated the effect of disease transmission on system dynamics. Our results show that, as the transmission rate of disease increases, the susceptible predator approaches extinction, whereas, on the other hand, when it declines, the susceptible predator shows robust oscillations while the infected approaches extinction. In both cases, the prey population demonstrates robust stability due to the prey refuge. Our findings show that the management of harvesting and the prey refuge can be effective ecological tactics for disease control and species protection under stochastic environmental effects.

Keywords: stochastic predator–prey model, harvesting, prey refuge, persistence, extinction

PACS: 05.40.–a, 05.45.–a, 05.10.Gg

DOI: 10.1088/1674-1056/adf17f **CSTR:** 32038.14.CPB.adf17f

1. Introduction

Predator–prey interactions are at the core of ecological theory, playing a fundamental role in shaping population dynamics, regulating biodiversity, and maintaining the structural integrity of ecosystems due to their prevalence and ecological importance.[1] These relationships help to elucidate key processes such as population persistence, species survival, and the effects of environmental disturbances on community stability.[2] In recent decades, mathematical modeling has emerged as a vital approach for studying such complex ecological interactions. By abstracting biological processes into mathematical frameworks, particularly differential equation systems, researchers can explore nonlinear dynamics, threshold behavior, and long-term system trajectories that are difficult or even impossible to observe directly in nature.[3,4] Furthermore, many predator–prey models have been extended to incorporate the effects of infectious diseases, reflecting the fact that pathogens can significantly influence the behavior, reproduction, and mortality of both predators and prey, ultimately impacting ecosystem stability.[5–7] These eco-epidemiological models often require advanced tools such as stochastic differential equations, Lyapunov stability theory, and extinction/permanence analysis to rigorously analyze their behavior under uncertainty and perturbation.

One of the key ecological elements influencing predator–prey systems is the concept of prey refuge, a mechanism by which a fraction of the prey population evades predation either through access to physical shelters or through adaptive behaviors that reduce vulnerability.[8] The ecological and mathematical significance of the prey refuge has been widely recognized, with numerous studies showing that its inclusion in predator–prey models contributes to increased system stability by reducing oscillation amplitudes and dampening population fluctuations.[9,10] In addition, the prey refuge serves as a critical survival mechanism that can prevent predator extinc-

†Corresponding author. E-mail: alkhazan84@yahoo.com
‡Corresponding author. E-mail: huizhang@nwpu.edu.cn

© 2026 Chinese Physical Society and IOP Publishing Ltd. All rights, including for text and data mining, AI training, and similar technologies, are reserved.

tion under extreme environmental or biological stress.[11] Its integration into mathematical models improves their biological realism and predictive capacity, making them more representative of natural ecosystems and more effective in forming conservation and management strategies.

Harvesting plays a significant role in the maintenance of the balance and co-existence of species in ecological communities and has generated considerable attention among scientists in recent years. Harvesting impact on the dynamics of biological populations is an interesting and important research topic. Various kinds of harvesting approaches have been considered in ecological and eco-epidemiological models, such as constant harvesting,[12] proportional harvesting,[13] and nonlinear harvesting.[14] All of these methods offer new insights into the role of human management in maintaining population stability and resource resilience. Purnomo *et al.*[15] analyzed a model with regular harvesting of the susceptible prey population and elaborated on its ecological relevance. Similarly, Bairagi *et al.*[16] generalized the model by incorporating harvesting in both infected and susceptible prey populations. To introduce more realism into harvesting, Das *et al.*[13] introduced a proportional harvesting function in the form of cEx, where E is the harvesting effect and c is the catch-ability coefficient. x represents population density. This was particularly useful in studying the economic impacts of harvesting on fisheries. In a more complex scenario, Abdulghafour *et al.*[14] proposed a nonlinear harvesting function as $\frac{cEY}{l_1E+l_2Y}$, where Y is the predator population, c is the predator catch-ability rate, and l_1, l_2 are positive constants. This function represents the saturation effect commonly observed in real harvesting activities, in which effort and yield are not linearly interrelated due to capacity or resistance constraints in the environment. Recent studies have increasingly focused on the complex dynamics of predator–prey interactions under nonlinear harvesting. For example, in Ref. [17], the authors explored how harvesting aimed specifically at the predator population can affect the behavior of the system, particularly with respect to optimizing economic yield from biological resources. In general, incorporating various harvesting strategies into ecological models makes them more applicable to conservation, fisheries, and wildlife management, and allows the development of sustainable harvesting policies based on mathematical insight.

One of the key factors in describing predator–prey dynamics is the functional response of the predator to the prey population. It defines the rate at which a predator consumes prey per unit of time as a function of the abundance of the prey. In order to accurately describe the feeding behavior of predators under different ecological conditions, several functional responses have been developed. These functional responses illustrate how the rate of predation responds to changes in prey density at different levels of populations. The choice of a functional response is crucial since it plays an important role in determining the stability and bifurcation characteristics of the ecological community. Various types of functional responses have been proposed, each depending on biological realism and empirical observation. These include the Holling type I,[18] Holling type II or Michaelis–Menten responses,[19] and the Holling type III and type IV responses.[20] In addition, more complex forms such as the ratio-dependent functional response,[21] the Beddington–DeAngelis response,[22] and the Crowley–Martin response[23] have been studied to incorporate predator interference and mutual predator interference. All of these play a central role in predicting the dynamical behaviors of predator–prey systems. However, among these types, the type II functional response, a saturating response, is widely accepted for representing the realistic consumption rate by predators at different prey densities.

A review of the literature indicates that numerous mathematical models have been developed, taking either harvesting or prey refuge individually to analyze the dynamics of predator–prey systems. However, these models cannot capture the complete ecological reality. Prey refuge is an ecological phenomenon in predator–prey systems, and its exclusion from the model may result in an unrealistic analysis of predator–prey systems. In addition to this, although a lot of work has been done on the introduction of harvesting strategies, little work can be found that combines both prey refuge and harvesting within the scenario of disease dynamics; even more surprisingly, no model has been developed which incorporates these two phenomena having disease among the predator population. Therefore, based on the work of Das,[24] which considered a predator–prey model with disease endemic to the predator population, this work proposes an extended and more biologically meaningful model. We also add prey refuge and harvesting, both of which are established in the literature for their significant influence on species persistence, population regulation, and ecosystem stability. The proposed model can be stated under the assumptions given in Section 2 as follows:

$$\begin{cases} \dfrac{\mathrm{d}X}{\mathrm{d}T} = rX\left(1-\dfrac{X}{K}\right) - \dfrac{X(1-\rho)(c_1Y+c_2Z)}{a_1+(1-\rho)X}, \\ \dfrac{\mathrm{d}Y}{\mathrm{d}T} = \dfrac{m_1c_1(1-\rho)XY}{a_1+(1-\rho)X} - d_1Y - \lambda_1YZ - h_yY, \\ \dfrac{\mathrm{d}Z}{\mathrm{d}T} = \dfrac{m_2c_2(1-\rho)XZ}{a_1+(1-\rho)X} + \lambda_1YZ - (d_1+\alpha_1)Z - h_zZ, \end{cases} \tag{1}$$

where the densities of prey, susceptible predator, and infected predator are indicated by X, Y, and Z, respectively, with respect to time T. K represents the carrying capacity, and r is the growth rate of the prey. The parameter c_1 represents the rate of consumption of prey by susceptible predators, while c_2 is the rate of consumption of prey by diseased predators. The half-saturation constant a_1 is the level of prey population at which predation is reduced to half of its maximum rate. The

parameters m_1 and m_2 represent the conversion rates of prey to susceptible and infected predators. The parameter d_1 represents the natural death rate of predators. The factor $(1-\rho)$ represents the prey refuge, which is controlled by the parameter ρ and h_y, h_z represents the harvesting in the susceptible predator and the infected predator, respectively. The parameter λ_1 captures the disease transmission rate from infected predators to susceptible ones. The parameter α_1 represents the extra mortality rate in predators as a result of infection.

For simplicity, system (1) can be converted into a non-dimensional form by using these transformations

$$x^p = \frac{X}{K}, \quad y^s = \frac{Y}{K}, \quad z^i = \frac{Z}{K}, \quad t = rT.$$

We non-dimensionalize time by defining $t = rT$, where T is dimensional time, and t is the corresponding dimensionless time variable. After suitable simplification, system (1) becomes

$$\begin{cases} \dfrac{\mathrm{d}x^p}{\mathrm{d}t} = x^p(1-x^p) - \dfrac{x^p(1-\rho)(\phi_1 y^s + \phi_2 z^i)}{1+l(1-\rho)x^p}, \\ \dfrac{\mathrm{d}y^s}{\mathrm{d}t} = \dfrac{\alpha\phi_1(1-\rho)x^p y^s}{1+l(1-\rho)x^p} - dy^s - \varepsilon y^s z^i - h_1 y^s, \\ \dfrac{\mathrm{d}z^i}{\mathrm{d}t} = \dfrac{\beta\phi_2(1-\rho)x^p z^i}{1+l(1-\rho)x^p} + \varepsilon y^s z^i - \pi z^i - h_2 z^i. \end{cases} \tag{2}$$

Here

$$\phi_1 = \frac{c_1 K}{r a_1}, \quad \phi_2 = \frac{c_2 K}{r a_2}, \quad l = \frac{K}{a_1}, \quad \alpha = \frac{m_1 K}{r a_1}, \quad d = \frac{d_1}{r},$$
$$\beta = \frac{\lambda_1 K}{r a_1}, \quad \pi = \frac{d_1 + \alpha_1}{r}, \quad \varepsilon = \frac{\lambda_1 K}{r}, \quad h_1 = \frac{h_y}{r}, \quad h_2 = \frac{h_z}{r}.$$

In addition to the ecological conditions discussed above, environmental perturbations are also responsible for affecting community structures and have become a focus of interest in ecological research.[25–27] Stochastic variations are ignored by traditional deterministic models, which assume that stochastic variations in large populations are negligible. In fact, the real success of a deterministic approach exists only when its predicted dynamics do not deviate even under the effect of environmental randomness. Recognizing the importance of these random disturbances, many researchers have developed stochastic models to better understand the behavior of single-species and multi-species populations under such conditions.[28–33] Liu and Wang[34] studied the stochastically asymptotic stability of the predator–prey system with Beddington–DeAngelis functional response under stochastic perturbations. Their results show that when the positive equilibrium of the deterministic model is globally stable, it will keep this stability in the stochastic model, provided that the noise is kept sufficiently small. In addition, Li and Wang[35] proposed a predator–prey model that incorporates the Beddington–DeAngelis functional response. To extend the analysis beyond a deterministic framework, a stochastic version of the model is explored, where random perturbations are introduced to certain parameters. Feng *et al.*[36] studied the combined impacts of infectious diseases and noise on predator–prey interactions. The analysis reveals that when environmental disturbances are low intensity, the population sizes tend to fluctuate around a stable equilibrium. However, when the intensity of these disturbances becomes too high, it can destabilize the system, ultimately leading to the extinction of one or both populations. Zhang *et al.*[37] examined the extinction and persistence conditions of predator populations in stochastic systems. Furthermore, Roy and Alam[38] showed that a high level of environmental noise along with fear-induced behavioral changes were capable of profoundly altering the extinction or persistence status of species. More recently, Sk and Pal[39] investigated an eco-epidemiological model with generalist predators and the interactive effects of fear, refuge, and harvesting under conditions of environmental uncertainty. A stochastic predator–prey model that incorporates diseases in the first prey was proposed by Gokila *et al.*[40] In their study, they established conditions for species permanence and extinction, providing a significant understanding of the system's long-term behavior under environmental influence. In addition, many epidemic models have been established that incorporate various types of noises. For detailed knowledge, the reader should refer to the works cited, such as Refs. [41–46]. These studies collectively demonstrate the richness and diversity of dynamics engendered through stochasticity in ecological systems and advocate stochastic modeling as the optimum method to represent real-world complexity.

To better characterize the nature of real ecosystems, we introduce random perturbations into the system (2) to simulate fluctuating environments and their influence on species survival and extinction episodes. However, previous work has independently studied phenomena such as prey refuge, harvesting, or stochasticity. To our knowledge, no stochastic predator–prey model has yet been constructed combining prey refuge and harvesting with a Holling type II functional response for a disease-infected predator population. This study bridges the gap by developing a comprehensive stochastic predator–prey model, providing novel insight into how disease processes influence ecological tactics and environmental stochasticity. Therefore, the system (2) takes the following form:

$$\begin{cases} \dfrac{\mathrm{d}x^p}{\mathrm{d}t} = \left[x^p(1-x^p) - \dfrac{x^p(1-\rho)(\phi_1 y^s + \phi_2 z^i)}{1+l(1-\rho)x^p}\right]\mathrm{d}t \\ \qquad + \sigma_1 x^p\,\mathrm{d}B_1(t), \\ \dfrac{\mathrm{d}y^s}{\mathrm{d}t} = \left[\dfrac{\alpha\phi_1(1-\rho)x^p y^s}{1+l(1-\rho)x^p} - dy^s - \varepsilon y^s z^i - h_1 y^s\right]\mathrm{d}t \\ \qquad + \sigma_2 y^s\,\mathrm{d}B_2(t), \\ \dfrac{\mathrm{d}z^i}{\mathrm{d}t} = \left[\dfrac{\beta\phi_2(1-\rho)x^p z^i}{1+l(1-\rho)x^p} + \varepsilon y^s z^i - \pi z^i - h_2 z^i\right]\mathrm{d}t \\ \qquad + \sigma_3 z^i\,\mathrm{d}B_3(t), \end{cases} \tag{3}$$

where $B_i(t)$ denotes typical Brownian motion and σ_i indicates the noise intensity with $(i = 1,2,3)$.[12] For basic definitions,

useful lemmas, and understanding of stochastic models, the reader is referred to Refs. [47,48].

This paper proposes a stochastic predator–prey model. Our research builds on some existing studies by including vital ecological and environmental considerations such as prey refuge, harvesting, white noise, and disease dynamics in predators. The prey refuge (hiding behavior) of prey is a natural phenomenon in ecology, without considering it, one cannot analyze the dynamics of the system effectively. Therefore, these conditions make the model more realistic and robust in describing the predator–prey interaction. The main contributions of this work are as follows.

Development of the stochastic predator–prey model: we develop a robust stochastic model that includes prey refuge and harvesting, white noise, and predator disease and delivers a more realistic description of ecological communities faced with random perturbations.

Global positive solution: we have shown that the model has a global positive solution which ensures the mathematical practicability and biological reliability of the model.

Persistence and extinction conditions: we establish conditions under which species persist or become extinct and significantly improve species persistence and ecosystem stability.

Numerical simulations: to confirm the theoretical results, we performed numerical solutions of our model based on the Milstein method. We examine the impact of noise and the effect of refuge and harvesting in predators on system dynamics, expanding applicability, and realism of our model toward the actual situation.

The organization of this paper is carefully designed so that a comprehensive and sequential analysis of model (3) can be carried out. Section 2 gives underlying biological assumptions that form the basis of the model, some basic definitions, and lemmas. Section 3 has an analysis of the existence and uniqueness of a positive global solution. Section 4 is all about exploring the conditions under which species exist or go extinct and providing recommendations on the long-term dynamics of the system. Section 5 describes the numerical computations of the model (3) and, finally, Section 6 consolidates the main findings and observations from the analytical and numerical studies.

2. Preliminaries

Here, we introduce some basic definitions that serve as the basis for the subsequent analysis of the dynamics of the model. We also introduce the principal assumptions on which the model is based. We begin by observing the following n-dimensional stochastic differential equation:

$$\mathrm{d}u(t) = \phi(u(t),t)\,\mathrm{d}t + \psi(u(t),t)\,\mathrm{d}B(t) \quad \text{for} \quad t \geq t_0. \tag{4}$$

Let $\mathcal{C}^{2,1}(\mathbb{R}^n \times [t_0,\infty);\mathbb{R}_+)$ be the set of all nonnegative functions $V(u,t)$ defined on $\mathbb{R}^n \times [t_0,\infty)$ so that they are continuously twice differentiable in u and differentiable in t. Using the differential operator defined in Ref. [47]

$$L = \frac{\partial}{\partial t} + \sum_{i=1}^{n} \phi_i(u,t)\frac{\partial}{\partial u_i} + \frac{1}{2}\sum_{i,j=1}^{n} [\psi^{\mathrm{T}}(u,t)\psi(u,t)]_{ij}\frac{\partial^2}{\partial u_i \partial u_j}.$$

When L affects a function $V \in \mathcal{C}^{2,1}(\mathbb{R}^n \times [t_0,\infty);\mathbb{R}_+)$, then

$$LV(u,t) = V_t(u,t) + V_u(u,t)f(u,t) + \frac{1}{2}\mathrm{tr}\left[g^{\mathrm{T}}(u,t)V_u u(u,t)g(u,t)\right],$$

where $V_t = \frac{\partial V}{\partial t}$, $V_u = \left(\frac{\partial V}{\partial u_1},\ldots,\frac{\partial V}{\partial u_n}\right)$, and $V_u u = \left(\frac{\partial^2 V}{\partial u_i \partial u_j}\right)_{n\times n}$.

Applying Itô's formula, when $u(t) \in \mathbb{R}^n$, we have

$$\mathrm{d}V(u(t),t) = LV(u(t),t)\,\mathrm{d}t + V_u(u(t),t)\,g(u(t),t)\,\mathrm{d}B(t).$$

Definition 1[49] The model (4) solution $u(t)$ is referred to as having stochastic permanence when, for any $\varepsilon \in (0,1)$, there exists positive constants $\eta = \eta(\varepsilon)$ and $Y = Y(\varepsilon)$ so that, given any initial value $u_0 \in \mathbb{R}^3_+$, the solution $u(t)$ to model (4) possesses the following properties:

$$\liminf_{t\to\infty} \mathbb{P}\{|u(t)| \geq \eta\} \geq 1-\lambda,$$
$$\liminf_{t\to\infty} \mathbb{P}\{|u(t)| \leq Y\} \geq 1-\lambda.$$

Lemma 1 The following inequality holds:

$$m \leq 2(m+1-\log(m)) - (4-2\log 2), \quad \forall m > 0.$$

The proof of the above inequality can be found in Ref. [50]. In Fig. 1, we present a numerical validation of this inequality.

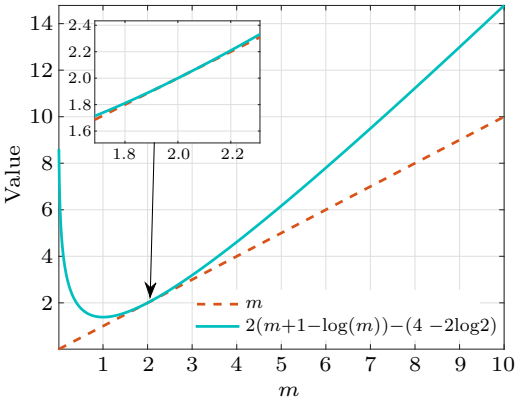


Fig. 1. Comparison of the left-hand side (LHS) and right-hand side (RHS) of the inequality for values of $m > 0$. The inequality holds if RHS $\geq$ LHS.

The construction of the proposed model is based on the following primary biological assumptions.

Assumption 1 The prey population grows logistically, in the absence of predation pressure, which signifies limited environmental resources and competition within the species.

Assumption 2 The model assumes that the disease is spreading exclusively within the predator population only. Transmission within the predator occurs through direct contact with each other.

Assumption 3 A portion of the prey population is always out of reach of predation by physical refuges or behavioral adaptations, known as prey refuge. It is a realistic ecological strategy where not all prey are accessible to predators and thus influences the feeding rate of the predator, as well as the population dynamics as a whole.

3. Existence of a positive solution

The model (3) describes the stochastic version of the proposed model. The solution provided by the model must be globally defined, positive, and bounded. The present section deals with the well-posedness of the model (3).

Theorem 1 For any initial value $(x_0^p, y_0^s, z_0^i) \in (\mathbb{R}^3_+)$, the model (3) has a unique solution $(x^p(t), y^s(t), z^i(t))$ and the solution will remain in $(\mathbb{R}^3_+)$ with probability one; so, for all $t \geq 0$, $(x^p(t), y^s(t), z^i(t)) \in (\mathbb{R}^3_+)$ almost surely.

Proof (see Ref. [40]) It is sufficient to demonstrate that $\tau = \infty$ is almost certainly true in order to demonstrate that the solution is global. Let n_0 be a large enough nonnegative integer so that (x_0^p, y_0^s, z_0^i) is contained in the closed ball $B(n_0) \subset \mathbb{R}^3_+$. For every $n \geq n_0$, we select and define the stop time as

$$\xi_n = \inf\left\{t \in [0, \xi_e) : x^p(t) \notin \left(\frac{1}{n}, n\right), y^s(t) \notin \left(\frac{1}{n}, n\right), z^i(t) \notin \left(\frac{1}{n}, n\right)\right\},$$

where $\inf \emptyset = \infty$ ($\emptyset$ is the empty set). Clearly, ξ_n is increasing as $n \to \infty$. Let $\xi_\infty = \lim_{n\to\infty} \xi_n$; then $\xi_\infty \leq \xi_e$ almost surely. If $\xi_\infty = \infty$ is indeed true, then $\xi_e = \infty$ almost surely. If this assertion is false, that is, $\xi_\infty \neq \infty$, then there are two constants $T > 0$ and $\varepsilon \in (0,1)$ such that

$$P\{\xi_\infty \leq T\} > \varepsilon. \tag{5}$$

Thus, by denoting $\Theta_n = \{\xi_n \leq T\}$, there is an integer $n_1 \geq n_0$ such that, for all $n \geq n_1$,

$$P\{\xi_n \leq T\} \geq \varepsilon. \tag{6}$$

Define a C^3 function $V : \mathrm{Int}(\mathbb{R}^3_+) \to \mathrm{Int}(\mathbb{R}^+ 3)$ by

$$V(x^p, y^s, z^i) = (x^p - c - c\log x^p) + k_1(y^s - 1 - \log y^s) + (z^i - 1 - \log z^i).$$

Here, c is constant and will be determined later. Applying Itô's formula to V, we obtain

$$d(V) = L(v)\,\mathrm{d}t + \sigma_1(x^p - c) + k_1\sigma_2(y^s - 1) + \sigma_3(z^i - 1)),$$

by the definition of operator L, we have

$$\begin{aligned} L(v) = {} & (x^p - c)\left(1 - x^p - \frac{(1-\rho)(\phi_1 y^s + \phi_2 z^i)}{1 + l(1-\rho)x^p}\right) \\ & + k_1(y^s - 1)\left(\frac{\alpha\phi_1(1-\rho)x^p}{1 + l(1-\rho)x^p} - d - \varepsilon - h_1\right) \\ & + (z^i - 1)\left(\frac{\beta\phi_2(1-\rho)x^p}{1 + l(1-\rho)x^p} + \varepsilon y^s - \pi - h_2\right) \\ & + \frac{c\sigma_1^2}{2} + \frac{k_1\sigma_2^2}{2} + \frac{\sigma_3^2}{2}. \end{aligned}$$

After differentiating with some simplification, the positivity of $x^p(t), y^s(t), z^i(t)$ will be

$$\begin{aligned} & \leq x^p - (x^p)^2 - \frac{x^p(1-\rho)(\phi_1 y^s + \phi_2 z^i)}{1 + l(1-\rho)x^p} - c + cx^p + \frac{c(1-\rho)(\phi_1 y^s + \phi_2 z^i)}{1 + l(1-\rho)x^p} + \frac{\alpha\phi_1 k_1(1-\rho)x^p y^s}{1 + l(1-\rho)x^p} \\ & \quad - k_1 d y^s - \varepsilon k_1 y^s - h_1 k_1 y^s - \frac{\alpha\phi_1 k_1(1-\rho)x^p}{1 + l(1-\rho)x^p} + k_1 d + k_1\varepsilon + k_1 h_1 + \frac{\beta\phi_2(1-\rho)x^p z^i}{1 + l(1-\rho)x^p} + \varepsilon y^s z^i \\ & \quad - \pi z^i - h_2 z^i + k_1\varepsilon - \frac{\beta\phi_2(1-\rho)x^p z^i}{1 + l(1-\rho)x^p} - \varepsilon y^s + \pi + h_2 + \frac{1}{2}(c\sigma_1^2 + k_1\sigma_2^2 + \sigma_3^2) \\ & \quad + \sigma_1(x^p - c)\,\mathrm{d}B_1 + k_1\sigma_2(y^s - 1)\,\mathrm{d}B_1 + \sigma_3(z^i - 1)\,\mathrm{d}B_3, \\ & \leq \left[(1+c)x^p + \frac{\alpha k_1\phi_1 y^s}{l} + \frac{\beta\phi_2 z^i}{l} + \frac{c\phi_1}{l} + \frac{c\phi_2}{l} + k_1 d + k_1\varepsilon + k_1 h_1 + \pi + h_2\right] dt \\ & \quad + \frac{1}{2}(c\sigma_1^2 + k_1\sigma_2^2 + \sigma_3^2) + \sigma_1(x^p - c)\,\mathrm{d}B_1 + k_1\sigma_2(y^s - 1)\,\mathrm{d}B_1 + \sigma_3(z^i - 1)\,\mathrm{d}B_3, \\ & \leq \left[\left(\frac{c\phi_1}{l} + \frac{c\phi_2}{l} + k_1 d + k_1\varepsilon + k_1 h_1 + \pi + h_2\right) + (1+c)x^p + \frac{\alpha k_1\phi_1 y^s}{l} + \frac{\beta\phi_2 z^i}{l}\right] dt \\ & \quad + \frac{1}{2}(c\sigma_1^2 + k_1\sigma_2^2 + \sigma_3^2) + \sigma_1(x - c)\,\mathrm{d}B_1 + k_1\sigma_2(y - 1)\,\mathrm{d}B_1 + \sigma_3(z - 1)\,\mathrm{d}B_3. \end{aligned}$$

Define positive constants as

$$b_1 = \frac{c\phi_1}{l} + \frac{c\phi_2}{l} + k_1 d + k_1\varepsilon + k_1 h_1 + \pi + h_2, \quad b_2 = 2\left((1+c) + \frac{\alpha k_1\phi_1}{l} + \frac{\beta\phi_2}{l}\right).$$

We use Lemma 1 in the form $m \le 2(m+1-\log(m))$, because the negative constant part has a negligible impact. Therefore, we have

$$(1+c)x^p + \frac{\alpha k_1 \phi_1 y^p}{l} + \frac{\beta \phi_2 z^i}{l} \le b_2 V(x^p, y^s, z^i).$$

Therefore,

$$\begin{aligned} \mathrm{d}V(x^p,y^s,z^i) &\le (b_1 + b_2 V(x,y,z))\,\mathrm{d}t + \sigma_1(x^p-1)\,\mathrm{d}B_1 \\ &\quad + \sigma_2(y^s-1)\,\mathrm{d}B_2 + \sigma_3(z^i-1)\,\mathrm{d}B_3, \\ &\le b_3(1+V(x^p,y^s,z^i))\,\mathrm{d}t + \sigma_1(x^p-1)\,\mathrm{d}B_1 \\ &\quad + \sigma_2(y^s-1)\,\mathrm{d}B_2 + \sigma_3(z^i-1)\,\mathrm{d}B_3, \end{aligned}$$

where $b_3 = \max(b_1, b_2)$. For $t_1 \le T$,

$$\begin{aligned} &\int_0^{\xi_n \wedge t_1} \mathrm{d}V(x^p,y^s,z^i) \\ &\le b_3 \int_0^{\xi_n \wedge t_1} (1+V(x^p,y^s,z^i))\,\mathrm{d}t \\ &\quad + \int_0^{\xi_n \wedge t_1} (x^p-1)\,\mathrm{d}B_1, \\ &\quad + \sigma_2 \int_0^{\xi_n \wedge t_1} (y^s-1)\,\mathrm{d}B_2 + \sigma_3 \int_0^{\xi_n \wedge t_1} (z^i-1)\,\mathrm{d}B_3, \end{aligned}$$

where $\xi_n \wedge t_1 = \min\{\xi_n, t_1\}$. By applying the properties of Itô's integral in conjunction with the preceding inequality, we have

$$\begin{aligned} &V(x^p(\xi_n \wedge t_1), y^s(\xi_n \wedge t_1), z^i(\xi_n \wedge t_1)) \\ &\le V(x^p(0), y^s(0), z^i(0)) \\ &\quad + b_3 \int_0^{\xi_n \wedge t_1} (1+V(x^p,y^s,z^i))\,\mathrm{d}t. \end{aligned}$$

After taking the expectations on each side of the aforementioned inequality, we apply Fubini's theorem to obtain

$$\begin{aligned} &\mathbb{E}V(x^p(\xi_n \wedge t_1), y^s(\xi_n \wedge t_1), z^i(\xi_n \wedge t_1)) \\ &\le V(x^p(0), y^s(0), z^i(0)) \\ &\quad + b_3 \mathbb{E} \int_0^{\xi_n \wedge t_1} (1+V(x^p,y^s,z^i))\,\mathrm{d}t \\ &\le (x^p(0), y^s(0), z^i(0)) + b_3 t_1 \\ &\quad + b_3 \mathbb{E} \int_0^{\xi_n \wedge t_1} V(x^p,y^s,z^i)\,\mathrm{d}t \\ &\le V(x^p(0), y^s(0), z^i(0)) + b_3 T \\ &\quad + b_3 \mathbb{E} \int_0^{t_1} V(x^p(\xi_n \wedge t), y^s(\xi_n \wedge t), z^i(\xi_n \wedge t))\,\mathrm{d}t \\ &\le V(x^p(0), y^s(0), z^i(0)) + b_3 T \\ &\quad + b_3 \int_0^{t_1} \mathbb{E}V(x^p(\xi_n \wedge t), y^s(\xi_n \wedge t), z^i(\xi_n \wedge t))\,\mathrm{d}t. \end{aligned}$$

Using Gronwall's inequality[47] and the aforementioned inequality, we have

$$\mathbb{E}V(x^p(\xi_n \wedge T), y^s(\xi_n \wedge T), z^i(\xi_n \wedge T)), \tag{7}$$

where

$$b_4 = (V(x^p(0), y^s(0), z^i(0)) + b_3 T)\,\mathrm{e}^{b_3 T}.$$

We obtain $P(\Theta_n) \ge \varepsilon$ from Eq. (7). In particular, there exists at least one of $x^p(\xi_n, \theta)$, $y^s(\xi_n, \omega)$ and $z^i(\xi_n, \omega)$ belonging to $\{n, \frac{1}{n}\}$, for $\theta \in \Theta_n$ and $V(x^p(\xi_n), y^s(\xi_n), z^i(\xi_n))$ is at least as small as $n+1-\log n$ and $\frac{1}{n}+1+\log n$. Thus,

$$V(x^p(\xi_n), y^s(\xi_n), z^i(\xi_n)) \ge (n+1-\log n) \wedge \left(\frac{1}{n}+1+\log n\right).$$

Hence, using Eqs. (5) and (7), we have

$$\begin{aligned} c_4 &\ge \mathbb{E}[I_{\Theta_n(\theta)} V(x^p(\xi_n,\theta), y^s(\xi_n,\theta), z^i(\xi_n,\theta))], \\ &\ge \varepsilon \left[(n+1-\log n) \wedge \left(\frac{1}{n}+1+\log n\right)\right], \end{aligned}$$

where the indicator function of Θ_n is $I_{\Theta_n(\theta)}$. Given $n \to \infty$, let $b_4 = \infty$, then $\infty > b_4$ yields $\infty > \infty$, which is a contradiction. Thus, $\xi_\infty = \infty$ almost surely. This completes the proof.

4. Persistence and extinction

This section covers the system's extinction and persistence under the following conditions:

(H1) $\max\{d + h_1, \pi + h_2\} + \frac{1}{2}\max\{\sigma_1^2, \sigma_2^2, \sigma_3^2\} < \min\{1, \alpha\phi_1(1-\rho), \beta\phi_2(1-\rho)\}$.

(H2) $1 - \frac{\sigma_1^2}{2} < 0$, $\frac{\alpha\phi_1}{l} - d - h_1 - \frac{\sigma_2^2}{2} < 0$, $\frac{\beta\phi_2}{l} + \varepsilon - \pi - h_2 - \frac{\sigma_3^2}{2} < 0$.

Theorem 2 Assume that condition (H1) is satisfied. Then the system (3) is stochastically permanent; that is, there are positive constants $\lambda \in (0,1)$ and $Y > 0$ such that

$$\liminf_{t\to\infty} P(|X(t)| \le Y) \ge 1 - \lambda.$$

Proof (see Ref. [40]) We first establish that for any given initial state $X(0) = (x^p(0), y^s(0), z^i(0)) \in \mathbb{R}^3_+$, the solution $X(t) = (x^p(t), y^s(t), z^i(t))$ remains well defined and satisfies

$$\limsup_{t\to\infty} \mathbb{E}\left(\frac{1}{|X(t)|^\tau}\right) \le N,$$

Here, τ denotes an arbitrary positive constant that satisfies the required condition

$$\begin{aligned} &\max\{d+h_1, \pi+h_2\} + \frac{\tau+1}{2}\max\{\sigma_1^2, \sigma_2^2, \sigma_3^2\} \\ &< \min\{1, \alpha\phi_1(1-\rho), \beta\phi_2(1-\rho)\}. \end{aligned} \tag{8}$$

Using Eq. (8), we take any arbitrary positive constant $\rho > 0$ that satisfies

$$\begin{aligned} &\tau < \min\{1, \alpha\phi_1(1-\rho), \beta\phi_2(1-\rho)\} - \rho \\ &-\tau\max\{d+h_1, \pi+h_2\} - \frac{\tau+1}{2}\max\{\sigma_1^2, \sigma_2^2, \sigma_3^2\} > 0. \end{aligned} \tag{9}$$

Define the Lyapunov function $V(x^p, y^s, z^i) = x^p + y^s + z^i$ for $(x^p, y^s, z^i) \in \mathbb{R}^3_+$ and let

$$U(x^p, y^s, z^i) = \frac{1}{V(x^p, y^s, z^i)}.$$

Then, using Itô's lemma, we obtain

$$\begin{aligned}
\mathrm{d}U(X) =& -U^2(X)\left[x^p\left((1-x^p)-\frac{(1-\rho)(\phi_1 y^s+\phi_2 z^i)}{1+l(1-\rho)x^p}\right)\right.\\
&+y^s\left(\frac{\alpha\phi_1(1-\rho)x^p}{1+l(1-\rho)x^p}-d-\varepsilon z^i-h_1\right)\\
&\left.+z^i\left(\frac{\beta\phi_2(1-\rho)x^p}{1+l(1-\rho)x^p}+\varepsilon y^s-\pi-h_2\right)\right]\mathrm{d}t\\
&+U^3(X)\left[(\sigma_1x^p)^2+(\sigma_2y^s)^2+(\sigma_3z^i)^2\right]\mathrm{d}t-U^2(X)\\
&\times\left[(\sigma_1x^p)\,\mathrm{d}B_1(t)+(\sigma_2y^s)\,\mathrm{d}B_2(t)+(\sigma_3z^i)\,\mathrm{d}B_3(t)\right]\\
=&\ \mathcal{L}U(X)\,\mathrm{d}t-U^2(W)(\sigma_1x^p\,\mathrm{d}B_1(t)\\
&+\sigma_2y^s\,\mathrm{d}B_2(t)+\sigma_3z^i\,\mathrm{d}B_3(t)).
\end{aligned}$$

The assumption H1 allows us to select a positive constant τ that satisfies Eq. (8). Once again, according to Itô's formula, we obtain

$$\begin{aligned}
\mathcal{L}(1+U(X))^\tau =&\ \tau(1+U(X))^{\tau-1}\mathcal{L}U(X)\\
&+\frac{1}{2}\tau(\tau-1)(1+U(X))^{\tau-2}U^4(X)\\
&\times[(\sigma_1x^p)^2+(\sigma_2y^s)^2+(\sigma_3z^i)^2].
\end{aligned}$$

Now, we can then select $\varepsilon>0$ small enough to satisfy Eq. (9); so

$$\begin{aligned}
&\mathcal{L}\mathrm{e}^{\varepsilon t}(1+U(X))^\tau\\
=&\ \varepsilon\,\mathrm{e}^{\varepsilon t}(1+U(X))^\tau+\mathrm{e}^{\varepsilon t}\mathcal{L}(1+U(X))^\tau\\
=&\ \mathrm{e}^{\varepsilon t}(1+U(X))^{\tau-2}\left[\varepsilon(1+U(X))^2+G\right],
\end{aligned}$$

where

$$\begin{aligned}
G=&-kU^2(X)\left[x^p\left((1-x^p)-\frac{(1-\rho)(\phi_1y^s+\phi_2z^i)}{1+l(1-\rho)x^p}\right)\right.\\
&+y^s\left(\frac{\alpha\phi_1(1-\rho)x^p}{1+l(1-\rho)x^p}-d-\varepsilon z^i-h_1\right)\\
&\left.+z^i\left(\frac{\beta\phi_2(1-\rho)x^p}{1+l(1-\rho)x^p}+\varepsilon y^s-\pi-h_2\right)\right]\\
&-kU^3(X)\left[x^p\left((1-x^p)-\frac{(1-\rho)(\phi_1y^s+\phi_2z^i)}{1+l(1-\rho)x^p}\right)\right.\\
&+y^s\left(\frac{\alpha\phi_1(1-\rho)x^p}{1+l(1-\rho)x^p}-d-\varepsilon z^i-h_1\right)\\
&\left.+z^i\left(\frac{\beta\phi_2(1-\rho)x^p}{1+l(1-\rho)x^p}+\varepsilon y^s-\pi-h_2\right)\right]\\
&+kU^3(X)\left[(\sigma_1x^p)^2+(\sigma_2y^s)^2+(\sigma_3z^i)^2\right]\\
&-\frac{k(k+1)}{2}kU^4(X)\left[(\sigma_1x^p)^2+(\sigma_2y^s)^2+(\sigma_3z^i)^2\right].
\end{aligned}$$

To estimate the upper bound of the expression $(1+U(X))^{\tau-2}[\varepsilon(1+U(X))^2+G]$, we use inequalities

$$\begin{aligned}
&\tau U^3(X)[(\sigma_1x^p)^2+(\sigma_2y^s)^2+(\sigma_3z^i)^2]\\
\le&\ \tau U(X)\max\{\sigma_1^2,\sigma_2^2,\sigma_3^2\},\\
&\frac{\tau(\tau+1)}{2}U^4(X)[(\sigma_1x^p)^2+(\sigma_2y^s)^2+(\sigma_3z^i)^2]\\
\le&\ \frac{\tau(\tau+1)}{2}U^2(X)\max\{\sigma_1^2,\sigma_2^2,\sigma_3^2\}.
\end{aligned}$$

Hence,

$$\begin{aligned}
&\mathcal{L}\mathrm{e}^{\varepsilon t}(1+U(X))^\tau\\
=&\ \mathrm{e}^{\varepsilon t}(1+U(X))^{\tau-2}\left[\varepsilon(1+U(X))^2+G\right],\\
\le&\ \mathrm{e}^{\varepsilon t}(1+U(X))^{\tau-2}\\
&\times\left\{\varepsilon+[2\varepsilon-\tau\min\{1,\alpha\phi_1(1-\rho),\beta\phi_2(1-\rho)\}\right.\\
&+\tau\max\{d+h_1,\pi+h_2\}\\
&+\tau\max\{\sigma_1^2,\sigma_2^2,\sigma_3^2\}\}U(X)\\
&+[\varepsilon-\tau\min\{1,\alpha\phi_1(1-\rho),\beta\phi_2(1-\rho)\}\\
&+\tau\max\{d+h_1,\pi+h_2\}\\
&\left.+\frac{\tau(\tau+1)}{2}\max\{\sigma_1^2,\sigma_2^2,\sigma_3^2\}\}U^2(X)\right\}.
\end{aligned}$$

We know from Eqs. (8) and (9) that a positive constant R exists so that $\mathcal{L}\mathrm{e}^{\varepsilon t}(1+U(X))^\tau\le R\mathrm{e}^{\varepsilon t}$ implies that

$$\mathbb{E}\left[\mathrm{e}^{\varepsilon t}(1+U(X))^\tau\right]\le(1+U(0))^\tau+\frac{R(\mathrm{e}^{\varepsilon t}-1)}{\varepsilon}.$$

Therefore,

$$\limsup_{t\to\infty}\mathbb{E}\left[U^\tau(X(t))\right]\le\limsup_{t\to\infty}\mathbb{E}\left[(1+U(X(t)))^\tau\right]\le\frac{R}{\varepsilon}.$$

Since

$$(x^p+y^s+z^i)^\tau\le3^\tau((x^p)^3+(y^s)^3+(z^i)^3)^{\frac{\tau}{3}}=3^\tau|X|^\tau,$$

where $X=(x^p,y^s,z^i)\in\mathbb{R}^3_+$. As a result,

$$\limsup_{t\to\infty}\mathbb{E}\left[\frac{1}{|X(t)|^\tau}\right]\le3^\tau\limsup_{t\to\infty}\mathbb{E}\left[U^\tau(X(t))\right]\le3^\tau\frac{R}{\varepsilon}=N.$$

Hence, for any $\lambda>0$, suppose $v=\left(\frac{\lambda}{N}\right)^{\frac{1}{\tau}}$. Applying Chebyshev's inequality, we obtain

$$\begin{aligned}
&P\left[|X(t)|<v\right]=P\left[|X(t)|^{-\tau}>v^{-\tau}\right]\\
\le&\ \mathbb{E}\left[|X(t)|^{-\tau}\right]/v^{-\tau}=v^\tau\mathbb{E}\left[|X(t)|^{-\tau}\right].
\end{aligned}$$

Specifically,

$$\liminf_{t\to\infty}P\{|X(t)|\ge v\}\ge1-\lambda.$$

Likewise, for small $\lambda>0$, we find that there exists $Y>0$ such that

$$\liminf_{t\to\infty}P\{|X(t)|\le Y\}\ge1-\lambda.$$

This proves the theorem.

Remark 1 To satisfy the inequality in assumption (H1), the largest squared value of σ_1^2, σ_2^2, and σ_3^2 should be minimized. Adjusting σ_i values so that the largest squared term is smaller than the smallest value on the RHS ensures that the inequality holds. As α, ϕ_1, and ρ increase, the RHS becomes stricter, requiring smaller values of σ_i for satisfaction. Please, see Fig. 2.

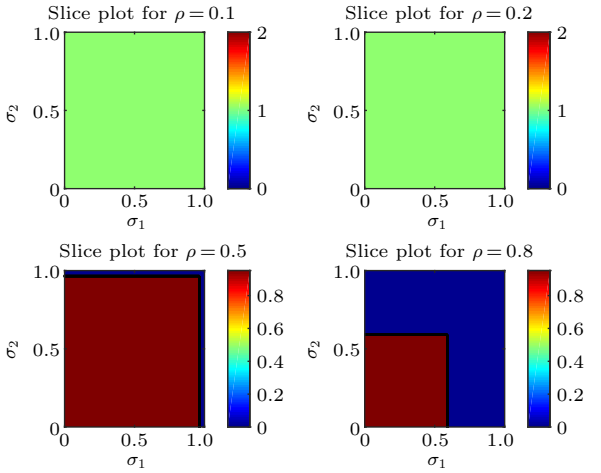


Fig. 2. Plots showing the region where the inequality in assumption (H1) holds for different values of ρ. Each subplot represents a 2D slice of the 3D region at a fixed σ_3 value. The color intensity indicates the region where the inequality is satisfied, with the color bar showing the intensity range.

Theorem 3 Suppose that condition (H2) is satisfied. Then for any initial value $X(0) = (x^p(0), y^s(0), z^i(0)) \in \mathbb{R}^3_+$, the solution $X(t) = (x^p(t), y^s(t), z^i(t))$ of the system (3) tends to extinction almost surely; that is,

$$\limsup_{t\to\infty} \frac{\ln|X(t)|}{t} < 0 \quad \text{implies} \quad \lim_{t\to\infty} X(t) = 0 \quad \text{a.s.}$$

Proof (see Ref. [40]) Initially, the Lyapunov function for the first equation $V_1 = \ln x^p$. Using Ito's formula, we obtain

$$\mathrm{d}(\ln x^p) = \left(1 - x^p - \frac{(1-\rho)(\phi_1 y^s + \phi_2 z^i)}{1 + l(1-\rho)x^p} - \frac{\sigma_1^2}{2}\right)\mathrm{d}t + \sigma_1 \mathrm{d}B_1(t).$$

Since the predation term is nonpositive, for the worst case of extinction, we set $y^s = z^i = 0$. When we integrate it from 0 to t, we obtain

$$\ln x^p(t) = \ln x^p(0) + \left(1 - \frac{\sigma_1^2}{2}\right)t + \sigma_1 \int_0^t \mathrm{d}B_1(t).$$

This leads to

$$\ln x^p(t) \le \ln x^p(0) + \left(1 - \frac{\sigma_1^2}{2}\right)t + \sigma_1 B_1(t).$$

Dividing by t on each side, we obtain

$$\frac{\ln x^p(t)}{t} \le \frac{\ln x^p(0)}{t} + \left(1 - \frac{\sigma_1^2}{2}\right) + \frac{\sigma_1 B_1(t)}{t}.$$

Now taking $t \to \infty$, and using the strong law of large numbers for a Brownian motion, that is,

$$\lim_{t\to\infty} \frac{B_1(t)}{t} = 0 \quad \text{almost surely},$$

we conclude

$$\limsup_{t\to\infty} \frac{\ln x^p(t)}{t} \le \left(1 - \frac{\sigma_1^2}{2}\right) < 0 \text{ almost surely.}$$

Also, define the Lyapunov function for the second equation $V_2 = \ln y^s$. Using Ito's formula, we obtain

$$\mathrm{d}(\ln y^s) = \left(\frac{\alpha\phi_1(1-\rho)x^p}{1 + l(1-\rho)x^p} - d - \varepsilon z^i - h_1 - \frac{\sigma_2^2}{2}\right)\mathrm{d}t + \sigma_2 \mathrm{d}B_2(t).$$

When we integrate it from 0 to t, we obtain

$$\ln y^s = \left(\frac{\alpha\phi_1}{l} - d - h_1 - \frac{\sigma_2^2}{2}\right)t + \sigma_2 \int_0^t \mathrm{d}B_2(t).$$

Thus,

$$\ln y^s \le \left(\frac{\alpha\phi_1}{l} - d - h_1 - \frac{\sigma_2^2}{2}\right)t + \sigma_2 B_2(t).$$

Dividing by t on each side, we obtain

$$\frac{\ln y^s(t)}{t} \le \left(\frac{\alpha\phi_1}{l} - d - h_1 - \frac{\sigma_2^2}{2}\right) + \frac{\sigma_1 B_2(t)}{t}.$$

Now taking $t \to \infty$, and using the strong law of large numbers for Brownian motion, we obtain

$$\limsup_{t\to\infty} \frac{\ln y^s(t)}{t} \le \left(\frac{\alpha\phi_1}{l} - d - h_1 - \frac{\sigma_2^2}{2}\right) < 0$$

almost surely.

Similarly, we introduce the Lyapunov function for the third equation $V_3 = \ln z^i$. Using Ito's formula, we obtain

$$\mathrm{d}(\ln z^i) = \left(\frac{\beta\phi_2(1-\rho)x^p}{1 + l(1-\rho)x^p} + \varepsilon y^s - \pi - h_2 - \frac{\sigma_3^2}{2}\right)\mathrm{d}t + \sigma_3 \mathrm{d}B_3(t).$$

When we integrate it from 0 to t, we obtain

$$\ln z^i = \left(\frac{\beta\phi_2}{l} + \varepsilon - \pi - h_2 - \frac{\sigma_3^2}{2}\right)t + \sigma_3 \int_0^t \mathrm{d}B_3(t).$$

Thus,

$$\ln z^i \le \left(\frac{\beta\phi_2}{l} + \varepsilon - \pi - h_2 - \frac{\sigma_3^2}{2}\right)t + \sigma_3 B_3(t).$$

Dividing by t on each side, we obtain

$$\frac{\ln z^i(t)}{t} \le \left(\frac{\beta\phi_2}{l} + \varepsilon - \pi - h_2 - \frac{\sigma_3^2}{2}\right) + \frac{\sigma_1 B_3(t)}{t}.$$

Now taking $t \to \infty$, and using the strong law of large numbers for Brownian motion, we obtain

$$\limsup_{t\to\infty} \frac{\ln z^i(t)}{t} \le \left(\frac{\beta\phi_2}{l} + \varepsilon - \pi - h_2 - \frac{\sigma_3^2}{2}\right) < 0$$

almost surely.

5. Numerical simulations

In this section, we present several numerical examples to validate the theoretical results derived earlier. To carry out these simulations, we apply the Milstein scheme to the system of stochastic differential equations described by the model in Eq. (3). The Milstein scheme is a second-order numerical method that approximates the solution of stochastic differential equations by considering both the drift (deterministic) and diffusion (stochastic) components. For the system of equations governing the evolution of the variables x_n^p, y_n^s, and z_n^i, the Milstein scheme can be expressed as follows:

$$x_{n+1}^p = \left[x_n^p(1-x_n^p) - \frac{x_n^p(1-\rho)\left(\phi_1 y_n^s + \phi_2 z_n^i\right)}{1+l(1-\rho)x_n^p}\right]\Delta t + \sigma_1 x_n^p\sqrt{\Delta t}\,\xi_n + \frac{\sigma_1^2}{2}x_n^p(\xi_n^2-1)\Delta t,$$

$$y_{n+1}^s = \left[\frac{\alpha\phi_1(1-\rho)x_n^p y_n^s}{1+l(1-\rho)x_n^p} - dy_n^s - \varepsilon y_n^s z_n^i - h_1 y_n^s\right]\Delta t + \sigma_2 y_n^s\sqrt{\Delta t}\,\xi_n + \frac{\sigma_2^2}{2}y_n^s(\xi_n^2-1)\Delta t,$$

$$z_{n+1}^i = \left[\frac{\beta\phi_2(1-\rho)x_n^p z_n^i}{1+l(1-\rho)x_n^p} + \varepsilon y_n^s z_n^i - \pi z_n^i - h_2 z_n^i\right]\Delta t + \sigma_3 z_n^i\sqrt{\Delta t}\,\xi_n + \frac{\sigma_3^2}{2}z_n^i(\xi_n^2-1)\Delta t,$$

where ξ_n represents standard normal random variables and Δt is the time step. The equations incorporate both deterministic interactions (drift terms) and stochastic fluctuations (diffusion terms). The additional correction term, $\frac{\sigma_i^2}{2}(\xi_n^2-1)\Delta t$, accounts for the nonlinearity in the diffusion, making the Milstein scheme more accurate than simpler methods such as Euler–Maruyama. These terms describe how the variables evolve under the combined influence of deterministic dynamics and random noise. Using this numerical method, we will explore the impact of various model parameters on the behavior of system and compare the results with the theoretical predictions.

We start our simulations with the initial conditions $x^p(0)=0.1$, $y^s(0)=0.1$, $z^i(0)=0.1$ and the time step $dt=0.001$ in the following examples.

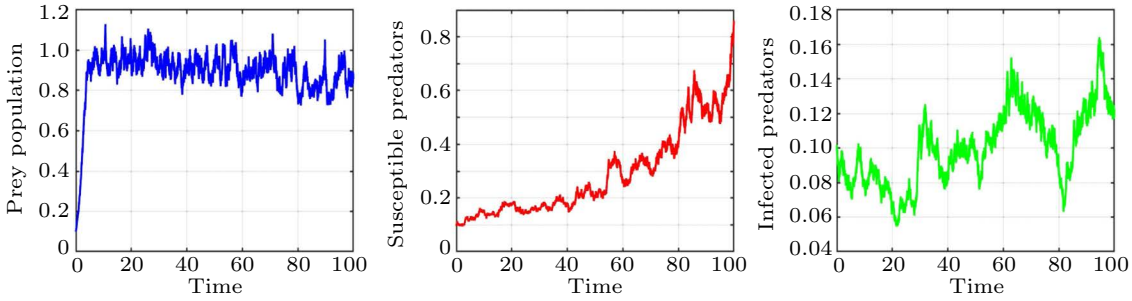


Fig. 3. Trajectories of model (3) by using the values of parameters in Example 1.

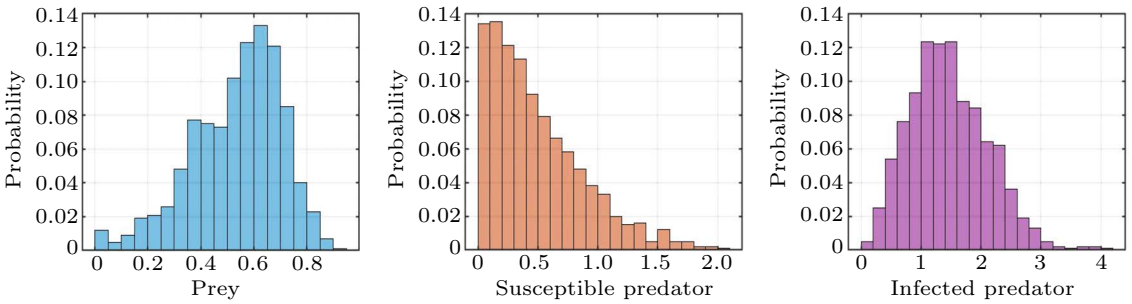


Fig. 4. Frequency histograms of model (3) by using the values of parameters in Example 1

Example 1 Using the following parameter values: $\phi_1 = 1.4$, $\phi_2 = 1.3$, $l = 3.5$, $\alpha = 0.45$, $\beta = 0.39$, $d = 0.04$, $\varepsilon = 0.02$, $\pi = 0.04$, $\rho = 0.8$, $h_1 = 0.003$, $h_2 = 0.001$, $\sigma_1 = 0.1$, $\sigma_2 = 0.1$, and $\sigma_3 = 0.1$, we verify that condition (H1) of Theorem 1 is satisfied, ensuring that the system exhibits persistent dynamics over time. This means that, under these parameter conditions, the populations of all species in the model remain positive and do not approach extinction. In Fig. 3, we illustrate the permanence of all species in the stochastic system described by Eq. (3). The figure shows that even under stochastic fluctuations, the system maintains a stable presence of all species, indicating that the interactions between the prey (x_n^p), susceptible (y_n^s), and infected (z_n^i) populations are sufficiently robust to avoid extinction. The system's ability to persist over time despite the randomness introduced by the noise terms is crucial for understanding the resilience of ecological systems under uncertainty. In addition, the corresponding frequency histogram in Fig. 4 provides further information on the long-term distribution of the species populations. From the histogram, we observe the statistical spread of each species' population, which reflects the varying effects of the stochastic terms in the model. The histogram also offers predictions on the most

likely population sizes, as well as the potential for extreme events (such as large fluctuations or population crashes) depending on the magnitude of the noise $(\sigma_1, \sigma_2, \sigma_3)$. This analysis suggests that, under the chosen parameter values, the system behaves in a way that supports the co-existence of all species, although the exact population levels may vary due to the random nature of the process. Adjusting the noise parameters (σ_i), we could predict how sensitive the system is to fluctuations. For example, higher values of σ_i could lead to greater population variability, which could increase the probability of occasional large deviations in species numbers. In contrast, smaller noise values could lead to more stable, predictable dynamics.

Example 2 When we increase the intensity of the noise to $\sigma_1 = 2.2$, while keeping all other parameters the same as in Example 1, Fig. 5 clearly illustrates a striking phenomenon: first, the prey population is wiped out, followed by the gradual collapse of the predator population. This sequence of events highlights the critical dependence of predators on the availability of prey for survival. As the prey population diminishes due to the stronger environmental stochasticity introduced by the increased noise intensity, predators are left without sufficient food resources, leading to their eventual extinction as well.

The result emphasizes the delicate balance within ecological systems and how external random fluctuations can severely disrupt population dynamics. In particular, it shows that increased environmental variability can destabilize populations that would otherwise persist in a deterministic setting. The extinction of prey acts as a tipping point that triggers a cascading effect throughout the food chain.

Example 3 For $\sigma_2 = 0.6$, with all other parameter settings remaining unchanged as in Example 1, the results confirm the validity of condition (H2) stated in Theorem 2. Specifically, Fig. 6 illustrates the extinction of the susceptible predator population over time.

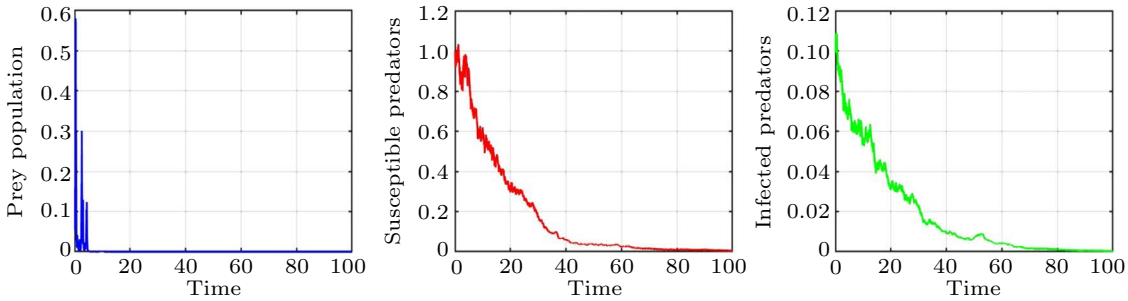


Fig. 5. Trajectories of model (3) by using the values of parameters in Example 2.

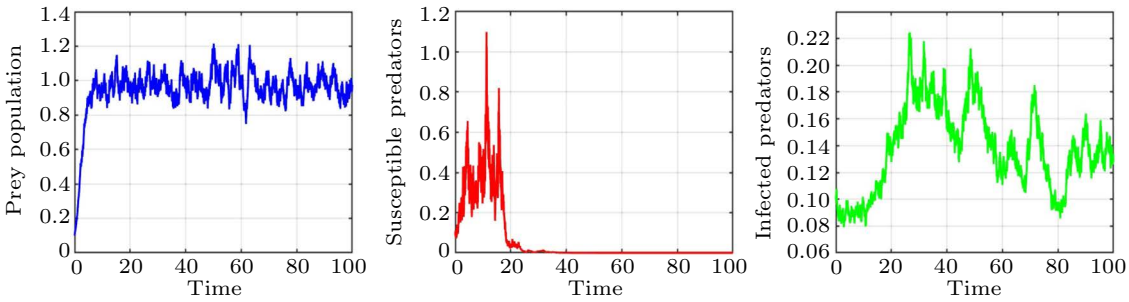


Fig. 6. Trajectories of model (3) by using the values of parameters in Example 3.

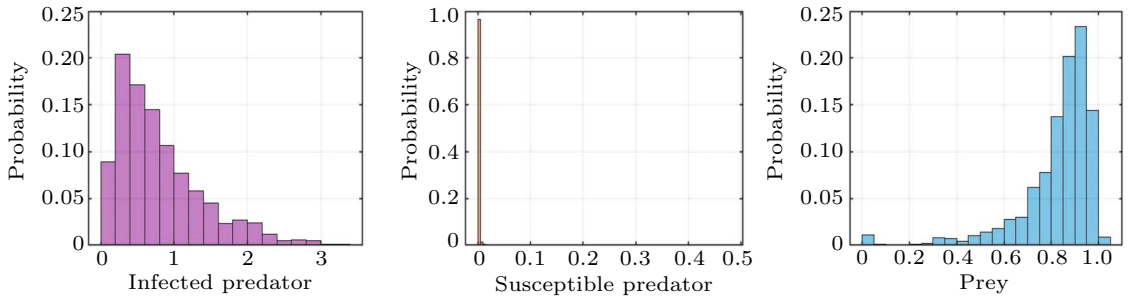


Fig. 7. Frequency histograms of model (3) by using the values of parameters in Example 3.

As the intensity of the noise σ_3 increases, stochastic perturbations significantly impact the dynamics of susceptible predators, leading to their eventual decline and disappearance. The extinction of susceptible predators in this setting highlights the crucial role that environmental fluctuations play in shaping population outcomes. In particular, it shows that even moderate noise can shift the long-term behavior of the system toward extinction scenarios that might not occur under

deterministic conditions. The corresponding frequency histogram, presented in Fig. 7, provides further statistical support for these findings, clearly showing that the final population sizes are heavily concentrated close to zero. This statistical evidence reinforces the observation of extinction and supports the theoretical predictions made under condition (H2).

Example 4 Similarly, for the same value of $\sigma_3 = 0.6$, while keeping all other parameters unchanged as in Example 1, the results further confirm the validity of condition (H2) stated in Theorem 2. In this case, Fig. 8 illustrates the extinction of the infected predator population over time. The increased intensity of noise σ_3 exerts a strong stochastic effect, not only on susceptible predators but also on infected ones, ultimately driving both groups towards extinction. This extinction phenomenon underlines the profound impact that environmental stochasticity can have on infected subpopulations within ecological systems. In particular, it demonstrates that infections within predator species can amplify vulnerability to random fluctuations, accelerating the decline compared to a healthy population. The corresponding frequency histogram shown in Fig. 9 further supports these results, indicating that the final population sizes are concentrated near zero with high probability.

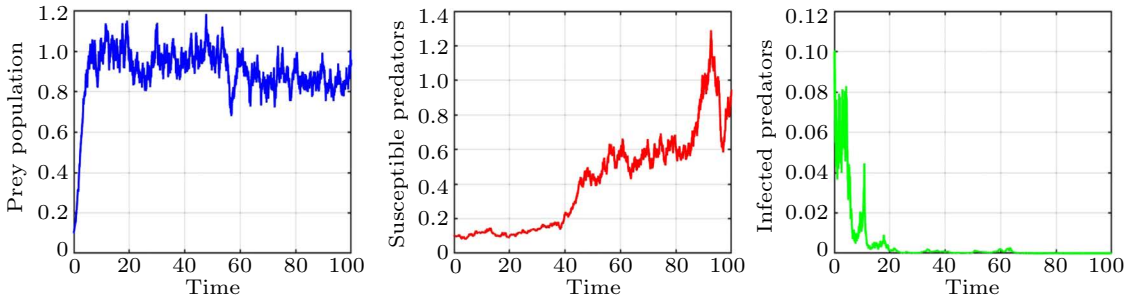


Fig. 8. Trajectories of model (3) by using the values of parameters in Example 4.

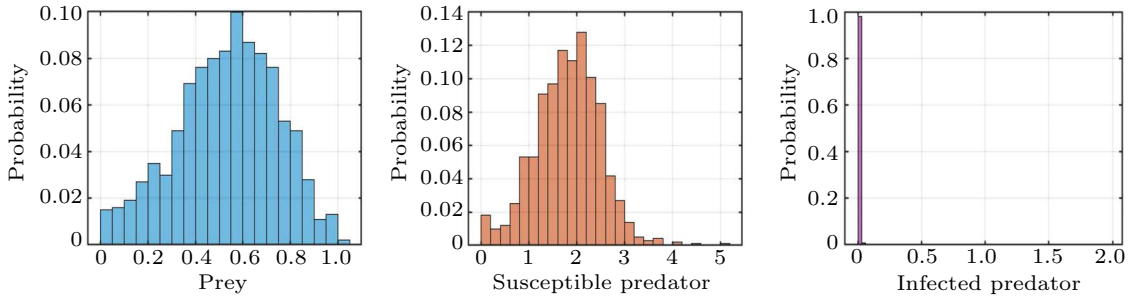


Fig. 9. Frequency histograms of model (3) by using the values of parameters in Example 4.

Example 5 In this example, we examine the combined impact of harvesting in predator and prey refuge on the dynamics of the system. Our objective is to understand how these two crucial ecological factors interact and influence the persistence or extinction of the species involved. To achieve this, we vary the prey refuge parameter from 0 to 0.9 and the harvesting rate from 0 to 0.3, as illustrated in Fig. 10, while keeping all other parameters unchanged as in Example 1. As observed in Fig. 10, the prey population and the susceptible predator population continue to exist, although exhibiting strong oscillatory behavior. This suggests that while both prey refuge and harvesting introduce significant pressures on the system, they do not immediately lead to the extinction of the main prey–predator interaction. Instead, the system experiences persistent fluctuations, possibly due to the dynamic balance between the protective effect of the refuge and the removal of individuals through harvesting. However, the infected predator population behaves differently under these conditions. Infected predators cannot withstand the combined stresses introduced by prey refuge and harvesting, and thus are driven toward extinction over the long term. This indicates that the infected subpopulation is more vulnerable compared to healthy predators, probably due to a compounded effect of limited prey access and additional mortality. Biologically, these findings reveal that prey refuge acts as a double-edged sword: Although it can protect prey and indirectly their healthy predators by preventing over-exploitation, it simultaneously makes life harder for already stressed populations, such as infected predators. Similarly, harvesting, although sustainable at moderate levels, can push vulnerable subpopulations to extinction when combined with other stressors.

Example 6 In this example, we examine the combined influence of prey refuge ρ and harvesting rates h_1 and h_2 on the stochastic dynamics of a prey–susceptible–infected predator system. From Figs. 11 and 12, we show that as the prey refuge ρ and the harvesting rates h_1 and h_2 increase, noticeable changes in the dynamical behavior of the system are observed. For lower values of refuge and harvesting, the prey and suscep-

tible predator populations exhibit strong stochastic oscillations around positive levels, while the infected predator population tends towards extinction. However, as ρ, h_1, and h_2 gradually increase, the dynamics of the system changes: the prey population becomes more resilient and stabilizes at higher levels due to the reduced predation pressure, while the populations of susceptible and infected predators decline and infected predators become more rapidly extinct. This transition highlights the crucial role of refuge and harvesting as ecological controls, prey refuge protects prey from over-exploitation, while harvesting reduces predator persistence.

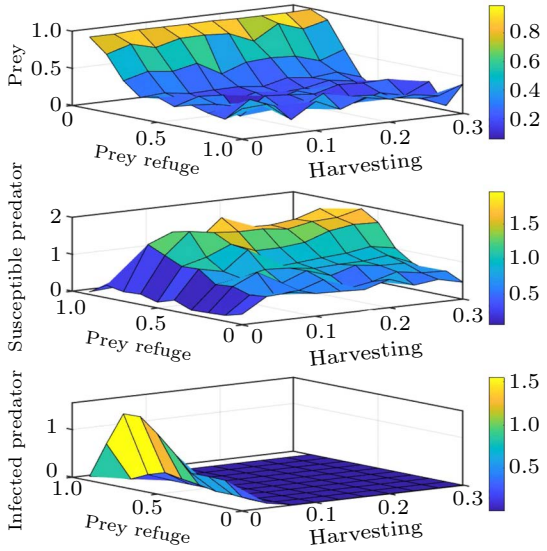


Fig. 10. Variational effect of prey refuge and harvesting of infected predator.

Example 7 In this example, we examine the effect of the disease transmission rate (ε) on the dynamics of the stochastic predator–prey system. From Figs. 13 and 14, we can see that the disease transmission rate significantly influences the dynamics of the system. In Fig. 13, we can observe that when the disease transmission rate increases, the susceptible population is heading towards extinct. It is because more susceptible predators become infected, and in the meanwhile the infected predators are increasing accordingly. On the other hand, in Fig. 14, we can clearly observe that when the disease transmission rate remains low, the susceptible population persists with strong oscillations while the infected persists is moving toward extinction. In addition, we can see the permanence of entire populations in Example 1 with a specific value of the transmission rate of diseases combining with prey refuge and harvesting.

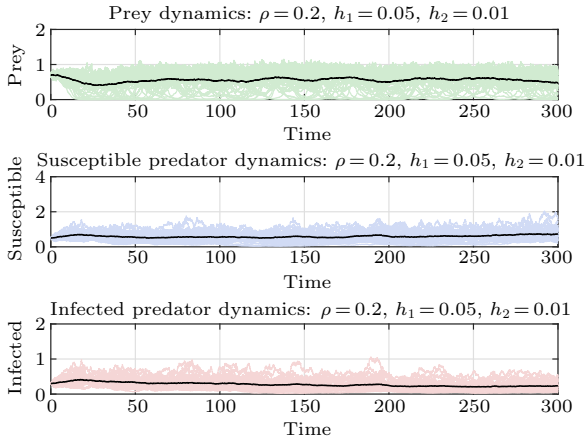


Fig. 11. Evolution of the prey population, susceptible predator population, and infected predator population under stochastic dynamics for the parameter set $(\rho, h_1, h_2) = (0.2, 0.05, 0.01)$. The light curves correspond to 50 individual stochastic trajectories, while the black bold curve represents the average behavior across simulations. The following parameter values are used throughout the simulation: $\phi_1 = 1.4$, $\phi_2 = 1.3$, $l = 3.5$, $\alpha = 0.45$, $\beta = 0.39$, $d = 0.04$, $\varepsilon = 0.02$, $\pi = 0.04$, $\sigma_1 = 0.1$, $\sigma_2 = 0.1$, and $\sigma_3 = 0.1$.

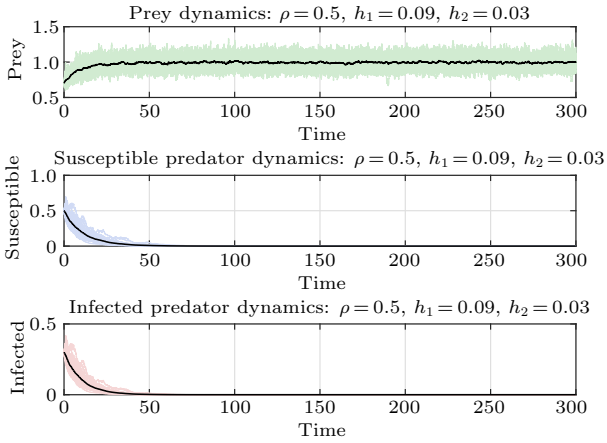


Fig. 12. Evolution of the prey population, susceptible predator population, and infected predator population under stochastic dynamics for the parameter set $(\rho, h_1, h_2) = (0.5, 0.09, 0.03)$. The light curves correspond to 50 individual stochastic trajectories, while the black bold curve represents the average behavior across simulations. The following parameter values are used throughout the simulation: $\phi_1 = 1.4$, $\phi_2 = 1.3$, $l = 3.5$, $\alpha = 0.45$, $\beta = 0.39$, $d = 0.04$, $\varepsilon = 0.02$, $\pi = 0.04$, $\sigma_1 = 0.1$, $\sigma_2 = 0.1$, and $\sigma_3 = 0.1$.

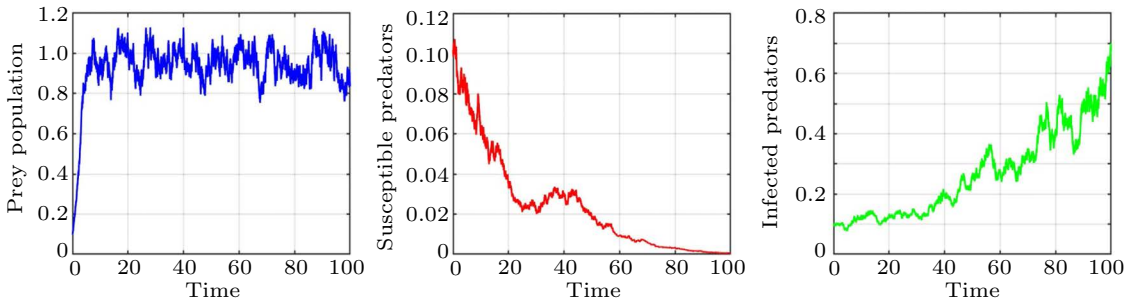


Fig. 13. Evolution of the prey population, susceptible predator population, and infected predator population under stochastic dynamics for the diseases transmission rate ($\varepsilon = 0.25$). The following parameter values are used throughout the simulation: $\phi_1 = 1.4$, $\phi_2 = 1.3$, $l = 3.5$, $\alpha = 0.45$, $\beta = 0.39$, $d = 0.04$, $\varepsilon = 0.02$, $\pi = 0.04$, $\sigma_1 = 0.1$, $\sigma_2 = 0.1$, and $\sigma_3 = 0.1$.

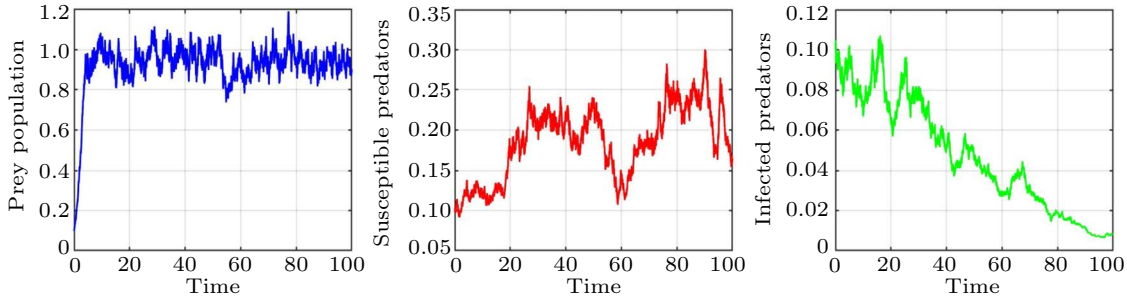


Fig. 14. Evolution of the prey population, susceptible predator population, and infected predator population under stochastic dynamics for the diseases transmission rate ($\varepsilon = 0.0003$). The following parameter values are used throughout the simulation: $\phi_1 = 1.4$, $\phi_2 = 1.3$, $l = 3.5$, $\alpha = 0.45$, $\beta = 0.39$, $d = 0.04$, $\varepsilon = 0.02$, $\pi = 0.04$, $\sigma_1 = 0.1$, $\sigma_2 = 0.1$, and $\sigma_3 = 0.1$.

6. Discussions and conclusion

In this paper, we introduced a novel stochastic eco-epidemiological model that incorporated both prey refuge and predator harvesting strategies. To our knowledge, this is the first study to explore a stochastic predator–prey system where infectious disease was confined solely to the predator population. The primary objective was to investigate how the varying levels of environmental noise, combined with the prey refuge and harvesting mechanisms, influenced the long-term dynamics of each population within system (3).

Our theoretical analysis established the existence of unique global positive solutions for all positive initial conditions. Furthermore, we characterized the conditions under which the populations exhibited persistence or extinction. In particular, under assumption (H1), the system was shown to be permanent, meaning that all populations survived indefinitely despite random fluctuations. Conversely, under assumption (H2), the system led to the extinction of populations, reflecting the impact of severe environmental disturbances or major epidemiological outbreaks.

Through extensive numerical simulations, we demonstrated that stochastic perturbations significantly affected the population dynamics: higher noise intensities facilitated extinction, while moderate noise levels supported co-existence through fluctuating persistence. In addition, our results highlighted the critical roles of prey refuge and harvesting. An increased level of prey refuge protected prey from predation, leading to stabilization and long-term persistence of the prey population. At the same time, intensified harvesting of the predator population, particularly infected predators, reduced the disease prevalence and altered the overall stability of the system. Specifically, we found that under appropriate combinations of refuge and harvesting rates, the prey and susceptible predator populations coexisted with strong oscillations, whereas the infected predator population tended toward extinction. In addition, we have investigated the effect of disease transmission on system dynamics. Our results show that, when the disease transmission rate increases, the susceptible predator tends toward extinction, and, on the other hand, when it decreases, the susceptible predators exist with strong oscillations while the infected is moving toward extinction. In both cases, the prey population shows strong stability due to the prey refuge.

Generally, the interaction between stochastic fluctuations, prey refuge, and harvesting strategies drove significant changes in the behavior of the ecosystem. Our findings suggested that controlled harvesting and management of prey refuge could serve as effective ecological tools for disease control and species conservation under random environmental influences.

Acknowledgements

This work was supported by the National Natural Science Foundation of China (Grant No. 32271554) and the Guangdong Basic and Applied Basic Research Foundation (Grant No. 2023A1515011501).

References

[1] Berryman A A 1992 *Ecology* **73** 1530
[2] Abrams P A 2000 *Annual Review of Ecology and Systematics* **31** 79
[3] Das K P, Samanta S, Biswas B and Chattopadhyay J 2014 *The Journal of Ecology* **108** 306
[4] Das K P 2015 *Journal of Dynamical and Control Systems* **21** 605
[5] Shaikh A A and Das H and Ali N 2018 *Journal of Applied Mathematics and Computing* **58** 235
[6] Ejaz A, Nawaz Y, Arif M S, Mashat D S and Abodayeh K 2022 *CMES-Computer Modeling in Engineering & Sciences* **132** 490
[7] Talib R H and Naji R k 2025 *Journal of Applied Mathematics* **2025** 8120929
[8] Ghosh J, Sahoo B and Poria S 2017 *Chaos, Solitons & Fractals* **96** 110
[9] Barman B and Ghosh B 2022 *International Journal of Modelling and Simulation* **42** 883
[10] Lazaar O and Serhani M 2023 *International Journal of Dynamics and Control* **11** 1934
[11] Boon J S, Keith S A, Exton D A and Field R 2023 *Global Ecology and Biogeography* **32** 1244
[12] Da S C, Michel I 2007 *Mathematical Biosciences* **205** 77
[13] Das T, Mukherjee R N and Chaudhuri K S 2009 *Applied Mathematical Modelling* **33** 2282
[14] Abdulghafour A S and Naji R K 2018 *Journal of Applied Mathematics* **1** 2952791
[15] Purnomo A S, Darti I and Suryanto A 2017 *AIP Conf. Proc.* (AIP Publishing) **1913** 020018
[16] Bairagi N, Chaudhuri S and Chattopadhyay J 2009 *Mathematical Biosciences* **217** 134
[17] Mandal S, Sk N, Tiwari P K and Chattopadhyay J 2024 *Chaos, Solitons & Fractals* **178** 114365
[18] Zou L and Zhang Z and Peng M 2025 *Pramana* **99** 16
[19] Cheru S L, Kebedow K G and Ega T T 2024 *Differential Equations and Dynamical Systems* 1
[20] Rahman M S, Islam M S and Sarwardi S 2025 *International Journal of Modelling and Simulation* **45** 20

[21] Hsu S B, Hwang T W and Kuang Y 2001 *Journal of Mathematical Biology* **42** 489
[22] Biswas S, Ahmad B and Khajanchi S 2023 *Mathematical Methods in the Applied Sciences* **46** 4184
[23] Upadhyay R K and Naji R K 2009 *Chaos, Solitons & Fractals* **42** 1337
[24] Das K P 2020 *Differential Equations and Dynamical Systems* **28** 295
[25] Sabbar Y, Aeshah A R 2024 *AIMS Math* **9** 18211
[26] Sabbar Y, Driss K 2023 *Mathematical Methods in the Applied Sciences* **46** 2455
[27] Sabbar Y, Asad k and Anwarud D 2022 *Mathematics* **10** 2262
[28] Liu M and Wang K 2009 *Ecological Modelling* **220** 1347
[29] Jiang D, Shi N Z and Zhao Y 2005 *Mathematical and Computer Modelling* **42** 651
[30] Ji C and Jiang D and Shi N Z 2011 *Journal of Mathematical Analysis and Applications* **377** 435
[31] Shah, S M A, Nie Y F, Din A, Alkhazzan A and Younas B 2024 *Chin. Phys. B* **33** 110203
[32] Shah S M A, Nie Y F, Din A and Alkhazzan A 2024 *Research Square* **33** 110203
[33] Shah, S M A, Nie Y F, Alkhazzan A, Tunç C and Din A 2024 *Journal of Taibah University for Science* **18** 2414523
[34] Liu M and Wang K 2011 *Communications in Nonlinear Science and Numerical Simulation* **16** 1114
[35] Li S and Wang X 2015 *Advances in Difference Equations* **2015** 1
[36] Feng Tao, Meng X Z, Zhang T and Qiu Z P 2020 *Qualitative Theory of Dynamical Systems* **19** 1
[37] Zhang X H, Li Yan and Jiang D Q 2017 *Nonlinear Dyn.* **87** 2011
[38] Roy J and Alam S 2020 *Physica A* **541** 123359
[39] Sk N and Pal S 2022 *Euro. Phys. J. Plus* **237** 138
[40] Gokila C, Sambath M, Balachandran K and Ma Y K 2023 *Journal of Biological Dynamics* **17** 2164803
[41] Alkhazzan A, Wang J G, Nie Y F, Khan H and Alzabut J 2024 *Chaos, Solitons & Fractals* **181** 114631
[42] Alkhazzan A, Wang J G, Nie Y F, Khan H and Alzabut J 2024 *Chaos* **34** 093119
[43] Alkhazzan A, Wang J G, Nie Y F, Khan H and Alzabut J 2023 *Alexandria Engineering Journal* **76** 557
[44] Alkhazzan A, Wang J G, Nie Y F, Khan H and Alzabut J 2024 *Mathematical Methods in the Applied Sciences* **47** 8748
[45] Alkhazzan A, Wang J G, Nie Y F, Khan H and Alzabut J 2023 *Chaos, Solitons & Fractals* **175** 113953
[46] Alkhazzan A, Wang J G, Nie Y F, Khan H and Alzabut J 2022 *Vaccines* **10** 1682
[47] Mao X 2007 *Stochastic differential equations and applications* 2nd Ed. (Glasgow: Elsevier) pp. 47–90
[48] Khasminskii R 2011 *Stochastic stability of differential equations* 2nd Ed. (USA: Springer Science & Business Media) pp. 43–58
[49] Li X Y and Mao X R 2009 *Discrete and Continuous Dynamical Systems-Series A* **24** 523
[50] Dalal N, Greenhalgh D and Mao X R 2008 *Journal of Mathematical Analysis and Applications* **341** 1084